

**Influence of pre-neutron fragment distributions  $Y(A, TKE)$   
and energy partition in fission on independent FPY,  
application for  $^{235}\text{U}(n_{th}, f)$**

**Anabella TUDORA**

**University of Bucharest, Faculty of Physics**

**ND-2022**

**15<sup>th</sup> Conference on Nuclear Data for Science and Technology**

**21 - 29 July 2022, California USA**

The **key role** in the calculation of post-neutron fragment distributions is played by

- the **distribution of pre-neutron (initial) fission fragments  $Y(A,TKE)$**
- the **modeling of prompt emission in fission** → strongly dependent on the **TXE partition**  
(the prompt neutron multiplicity being the most important quantity)  
in the majority of prompt emission model codes –  **$Y(A,TKE)$  are input data**

Our **deterministic** approaches **PbP** and **DSE** accomplish the statement of *S.Okumura, T.Kawano, P.Jaffke, P.Talou, S.Chiba* (e.g. *J.Nucl.Sci.Tech. 55 (9) 2018*), saying that:

“A deterministic treatment of prompt emission has the advantage to take into account the cases of fission fragment production with extremely small probabilities”, while “the MC technique never samples such cases in a reasonable computation time”.

In both PbP and DSE approaches **the deterministic construction of the fragmentation and TKE ranges leads to a number of initial fission fragment configurations  $(A,Z,TKE)$  of about 15000 – 17000** (for  $^{235}\text{U}(n_{\text{th}},f)$ )

**PbP** based on a **global treatment of sequential emission** →  $v(A,Z,TKE)$  as an average over the emission sequences →  **$A_p = A - v(A,Z,TKE)$  is not an integer**, this can constitute an **impediment** in the calculation of independent FPY etc.

**DSE treats each emission sequence** corresponding to an initial  $(A,Z,TKE)$  configuration → the number of emission sequences  $n(A,Z,TKE)$  being calculated,  **$A_p = A - n(A,Z,TKE)$  is an integer**. So that this approach **is more appropriate**, being used in this work.

for  $^{235}\text{U}(n_{\text{th}},f)$   $A = 76 - 160$ ; 5 Z per A as the nearest integer values below and above  $Z_p(A) = Z_{\text{UCD}}(A) - \Delta Z(A)$ ;  
 $p(Z,A)$  taken as Gaussians centered on  $Z_p(A)$ .  $\Delta Z(A)$ , rms(A) of Wahl → 215 fragmentations (430 initial fission fragments).  
For each fragmentation the TKE range is 120 – 200 with a step size of 2 MeV. The unphysical cases appearing especially at high TKE values (e.g. TXE < 0) are excluded. So that the  $(A,Z,TKE)$  number becomes of about 15000-17000.

## The influence on the distributions of post-neutron fragments is investigated for:

- 2 experimental Y(A,TKE) distributions of pre-neutron fission fragments, both measured at JRC-Geel, Belgium:
  - **Straede et al.** (*Nucl.Phys.A 462 (1987) 85-108*)
  - **Al-Adili et al.** (*Phys.Rev.C 86 (2012) 054601*)

The TXE partition methods are classified into 2 categories (differing as principle), i.e.

- methods based on different principles and assumptions about what is happening at scission (known as methods based on **modeling at scission**)
- methods which avoid what is happening at scission, the TXE sharing is based on **different parameterizations**

We have chosen one from each category:

- **our TXE partition based on modeling at scission** (*Tudora et al.*) used in PbP, DSE for each (A,Z,TKE) configuration:

i) the extra-deformation energy  $\Delta E_{\text{def}}^{(L,H)}$  as difference between the absolute deformation energy of a fragment at scission and at its full acceleration

ii) the statistical sharing of the available excitation energy at scission under the assumptions of statistical equilibrium at scission and level densities of nascent fragments in the F-G regime  $\rightarrow E_{\text{sciss}}^{(L,H)}$

iii) At full acceleration:  $E_{L,H}^* = \Delta E_{\text{def}}^{(L,H)} + E_{\text{sciss}}^{(L,H)}$

- **the TXE partition method based on the temperature ratio of complementary fully accelerated fragments**  $R_T = T_L/T_H$  which is an input parameter of the prompt emission code:

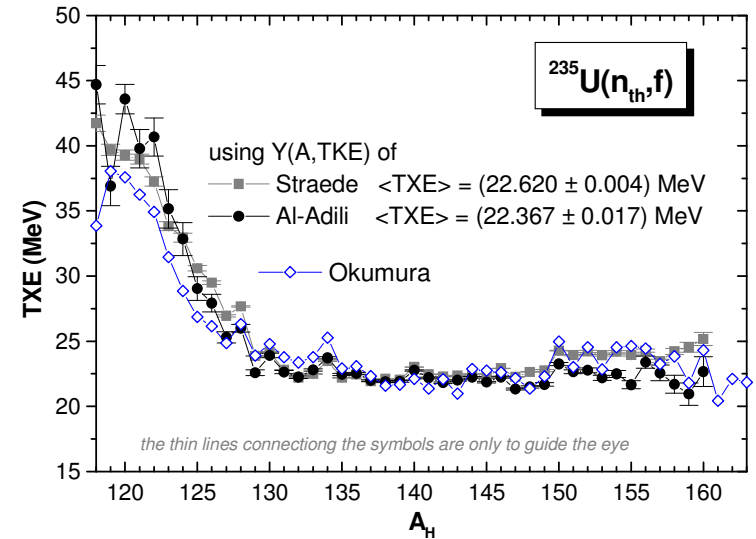
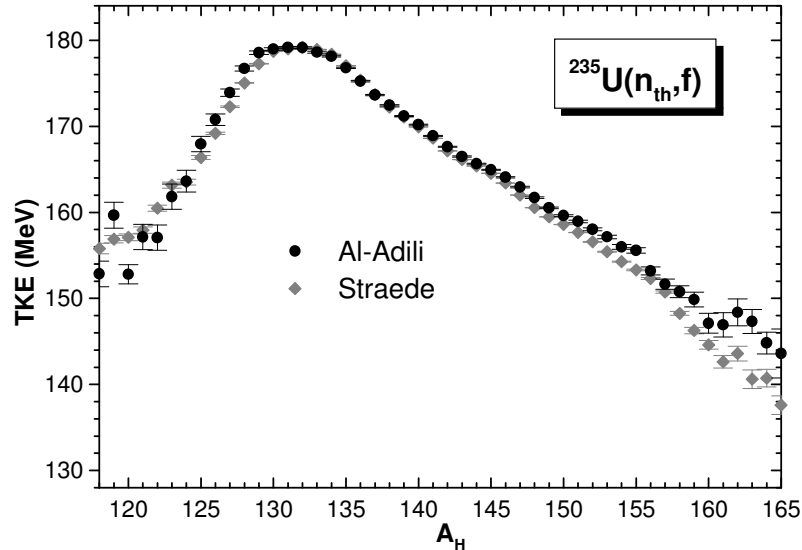
- $R_T$  as a function of A fitted to match the experimental  $v(A)$  data (used in the **CGMF code**),
- $R_T$  as an unique input value for all fragmentations (used in the **HF<sup>3</sup>D code**)

i.e.  $R_T = 1.2$  (*Okumura et al. J.Nucl.Sci.Tech. 55 (2018) 1009*)

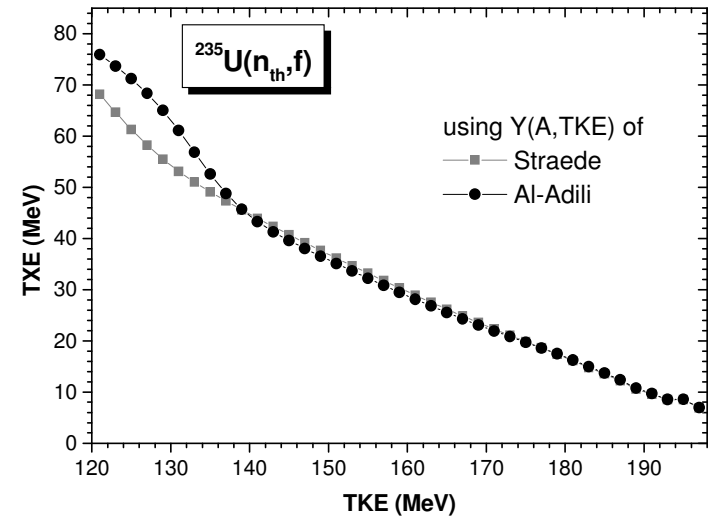
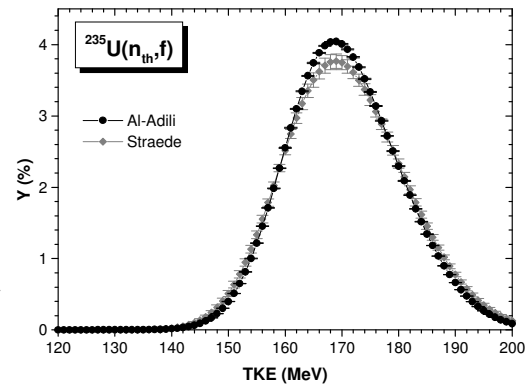
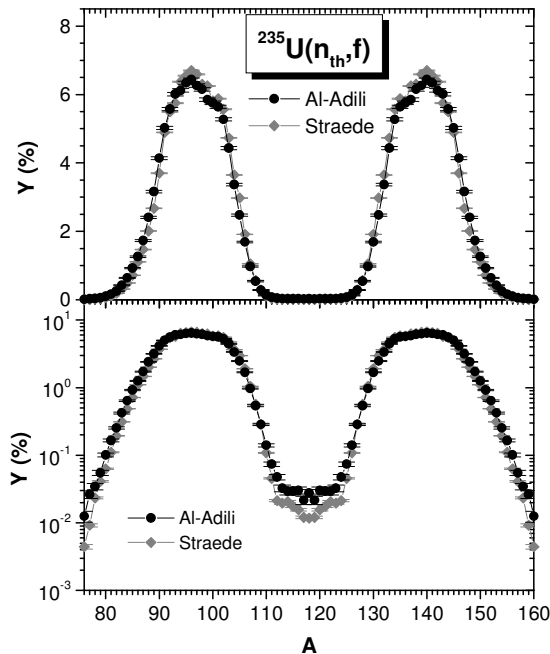
In the present work we have chosen  $R_T = 1.2$  (as in HF<sup>3</sup>D):

For each (A,Z,TKE):  $TXE = E_L^* + E_H^*$  shared according to  $R_T = 1.2$   $R_T = \sqrt{E_L^* a_H(E_H^*) / E_H^* a_L(E_L^*)}$

Differences between  $Y(A, TKE)$  data  $\rightarrow$  reflected in  $TXE(A)$  and  $TXE(TKE)$   
 better visible in the 2D representations

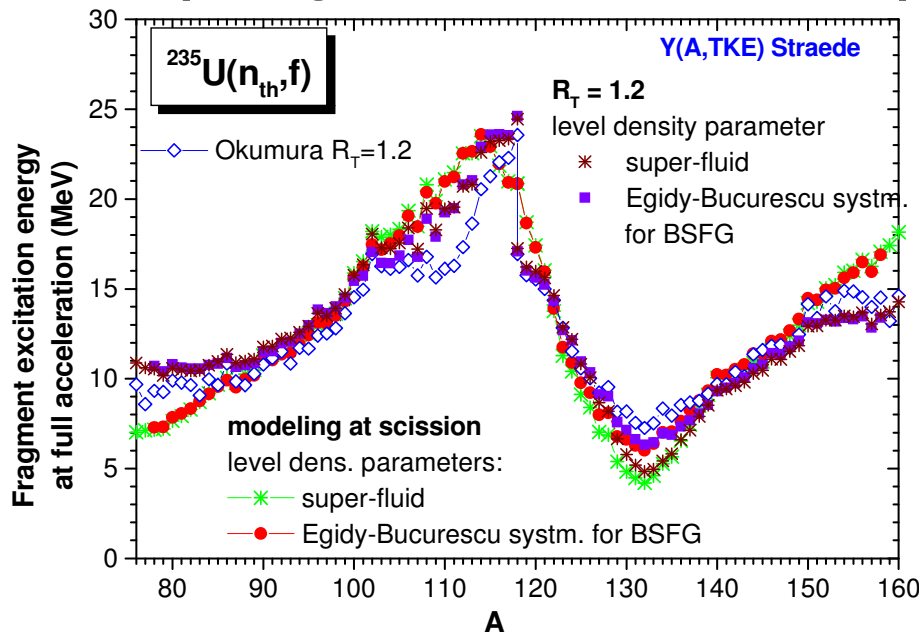


the differences in  $TKE(A)$  reflected in  $TXE(A)$  show the inverse correlation between  $TXE$  and  $TKE$



The differences in both  $Y(A)$  and  $Y(TKE)$  are reflected in the behaviour of  $TXE(TKE)$ .

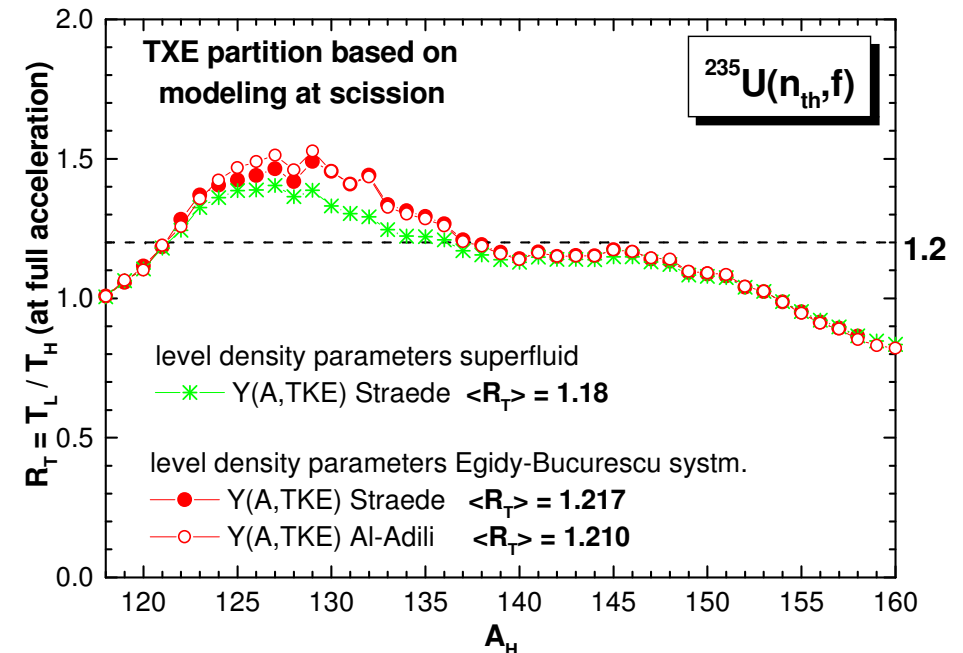
# Comparing the results of two TXE partition methods differing as principle



- Differences in  $E^*(A)$  due to different TXE partitions are visible over the entire A range (compare green and brown stars or full red and violet symbols)
- Some differences in  $E^*(A)$  due to different prescriptions for the level density parameter are visible at  $A_H$  around 132 (large negative shell corrections  $N=82, Z=50$ ) and at large asymmetric fragmentations.
- Differences in  $E^*(A)$  due to the same TXE partition (based on  $R_T=1.2$ ) applied in different models are also seen. HF<sup>3</sup>D (open symbols) and PbP / DSE (violet and brow symbols)

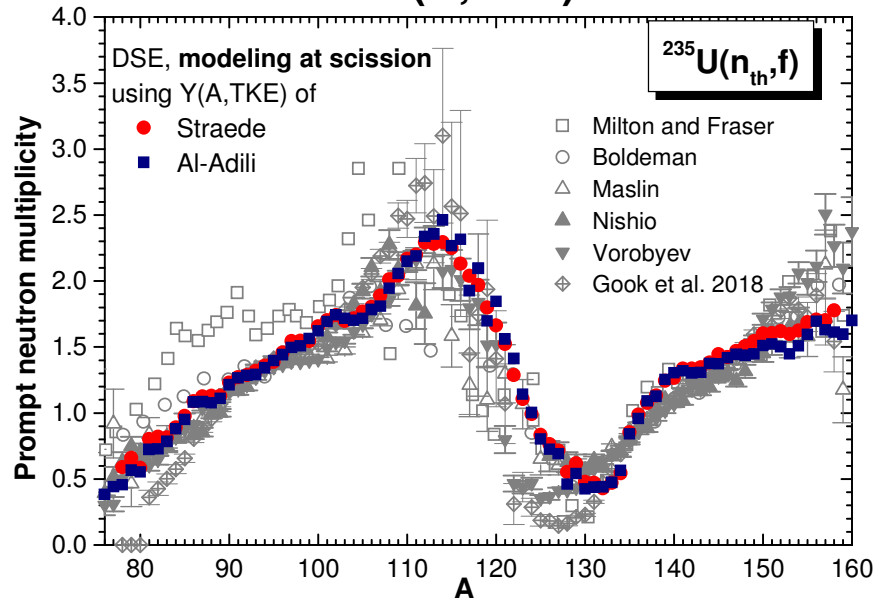
- i) based on modeling at scission  
the modeling at scission of Tudora et al. employed in PbP and DSE
- ← ii) avoiding what is happening at scission (using parameterizations)  
based on the input parameter  $R_T = T_L/T_H$  (employed in CGMF and HF<sup>3</sup>D)  
here  $R_T = 1.2$  (as in HF<sup>3</sup>D)

The value  $R_T=1.2$  found by Okumura et al. (giving the best agreement of HF<sup>3</sup>D results with exp. data) is very close to our  $\langle R_T \rangle$  resulting from the TXE partition based on modeling at scission. This can be considered as a validation in cross of both methods of TXE partition.

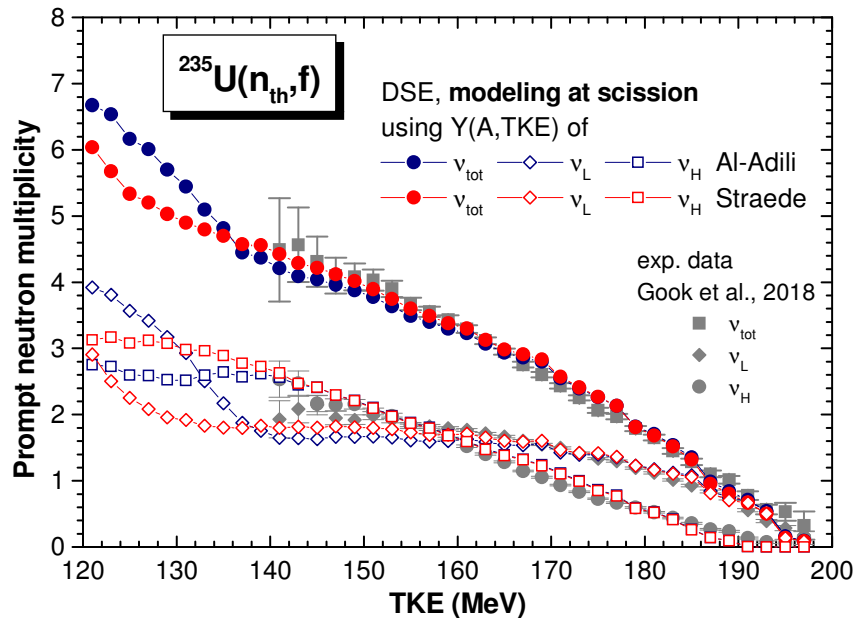
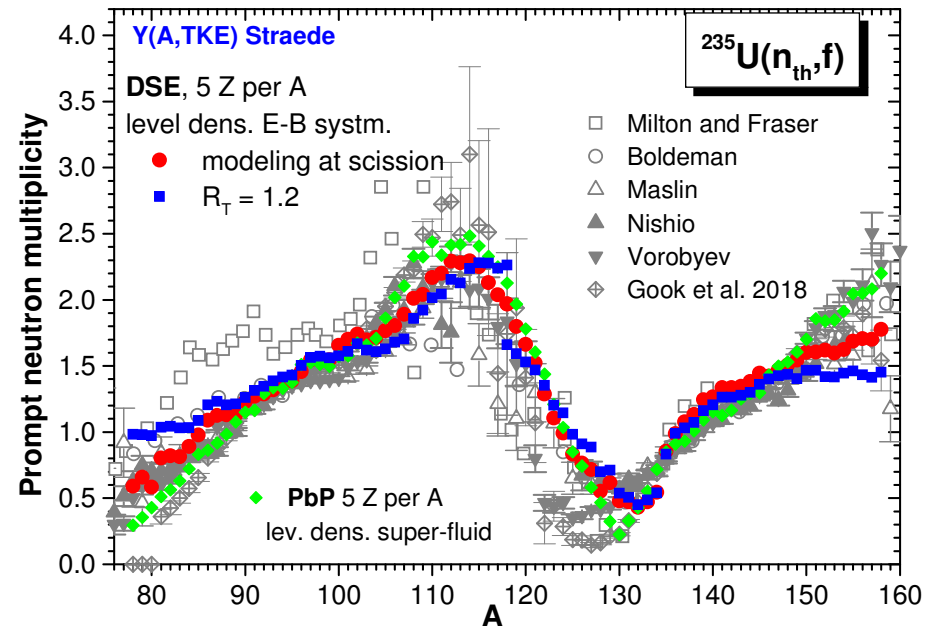


# Influence on the prompt neutron multiplicity (important giving $\lambda_p = A - \nu$ )

## of $Y(A, TKE)$



## of TXE partition method

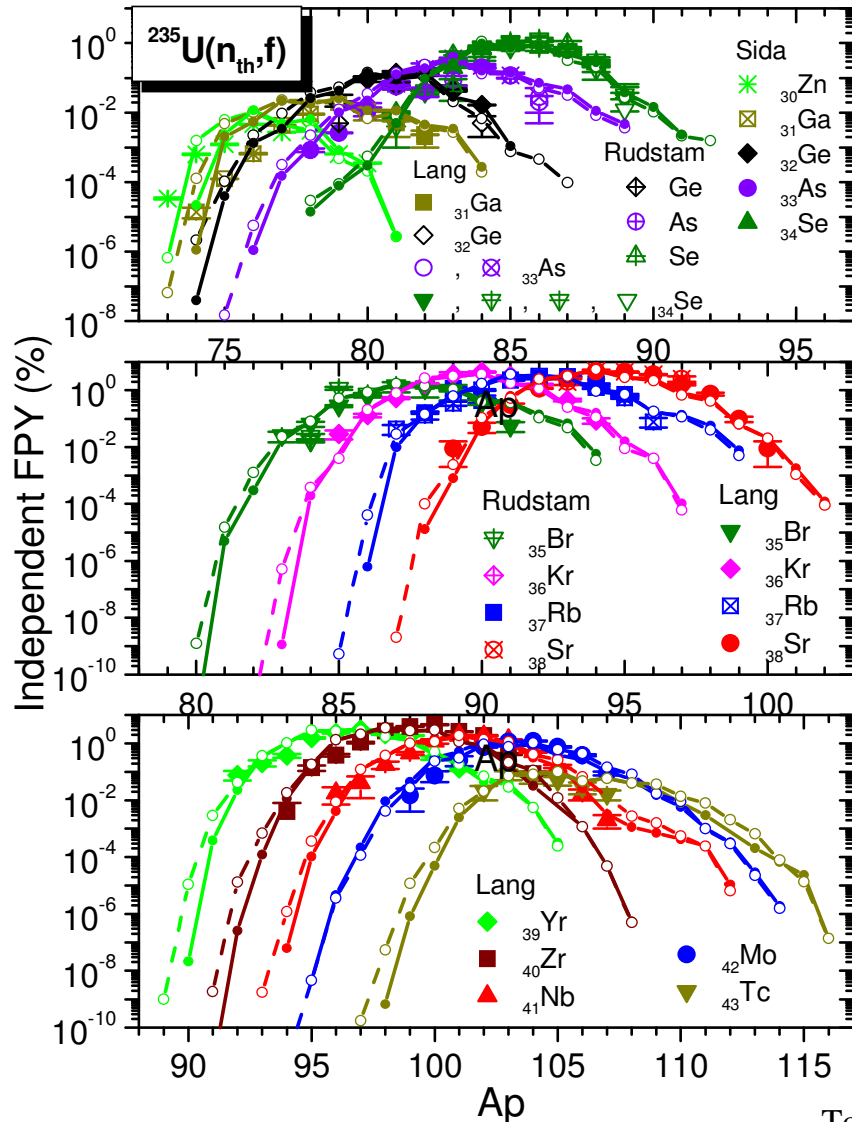


↑  
 The influence of TXE partition is visible only in  $\nu(A)$ , which is very sensitive to the TXE partition. Its influence on  $\nu(TKE)$  is almost insignificant.

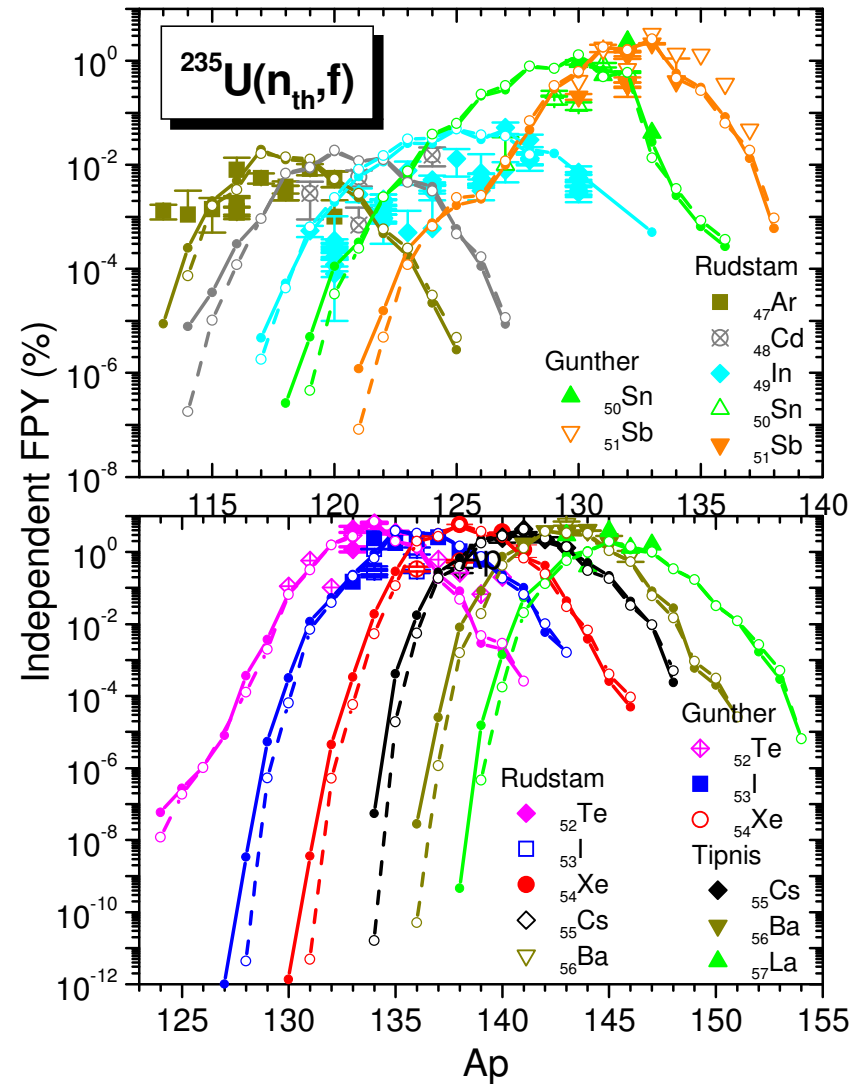
In the case of TXE partition based on modeling at scission the use of energy-dependent (super-fluid) or non-energy dependent (systematics) level density parameters is visible in  $\nu(A)$ , especially at  $A$  around 132 (due to the large negative shell corrections, magic nuclei  $N=82, Z=50$ ) – compare red and green symbols

# DSE results of $Y(Z, A_p)$ describe reasonably well the experim. data from EXFOR

$Y(Z, A_p)$  results using the TXE partition based on:  
 modeling at scission  $\rightarrow$  full *small circles* connected with solid line  
 $R_T = 1.2 \rightarrow$  open *small circles* connected with dashed lines



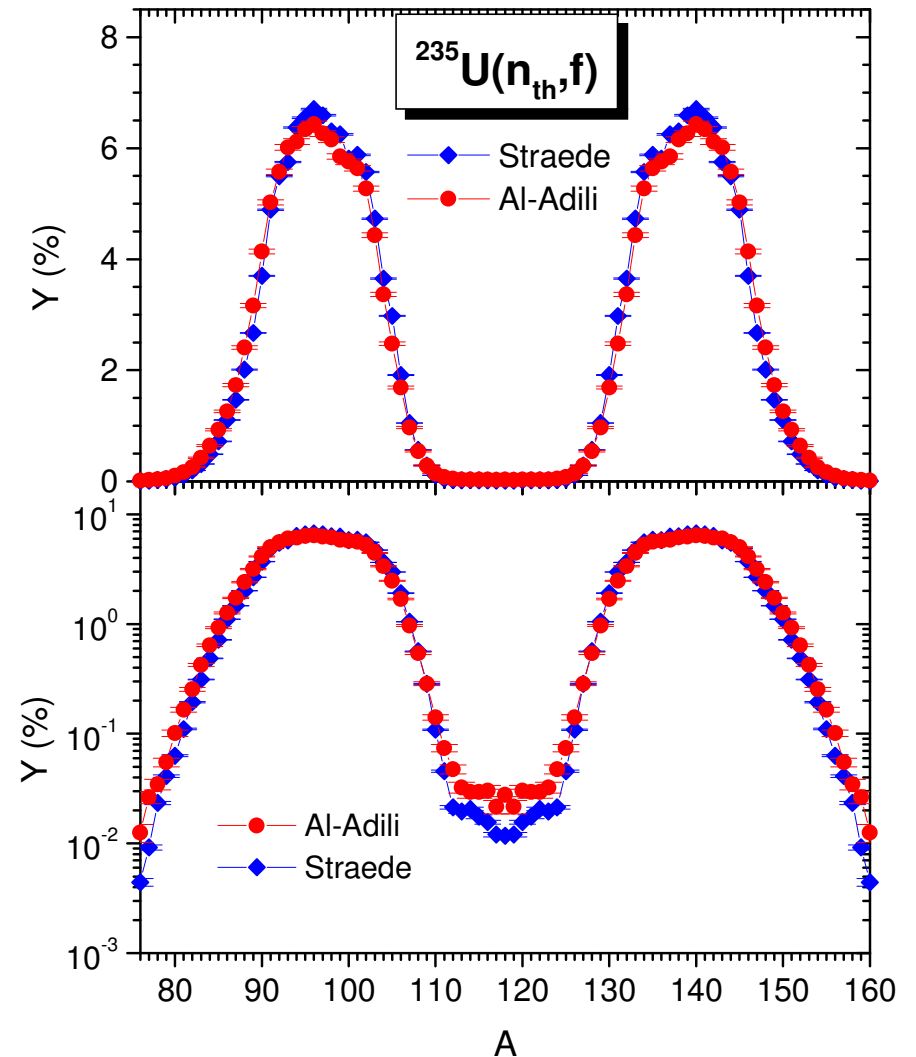
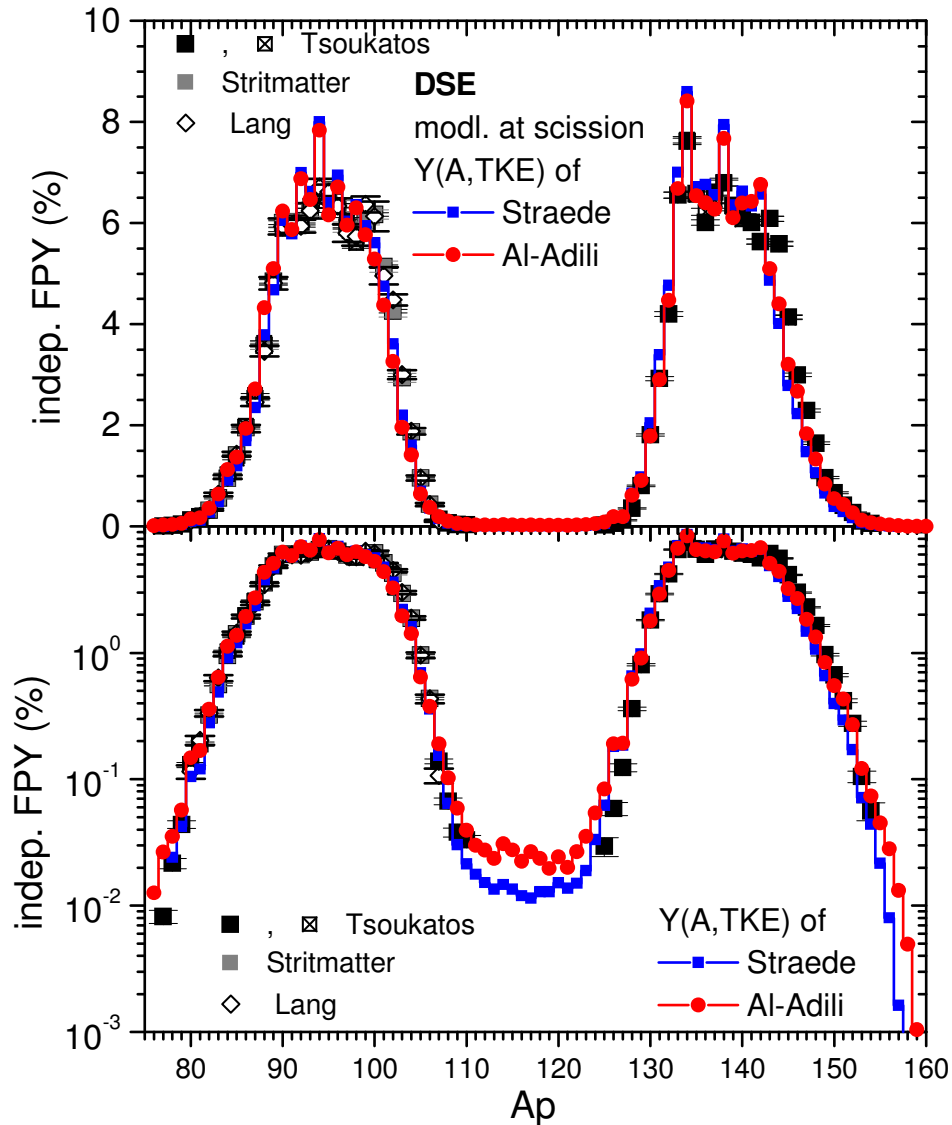
The  $Y(Z, A_p)$  results are plotted with the same color as the symbols of the experimental data for the respective charge number  $Z$



To avoid charged figures: exemplified for  $Y(A, \text{TKE})$  of Al-Adili



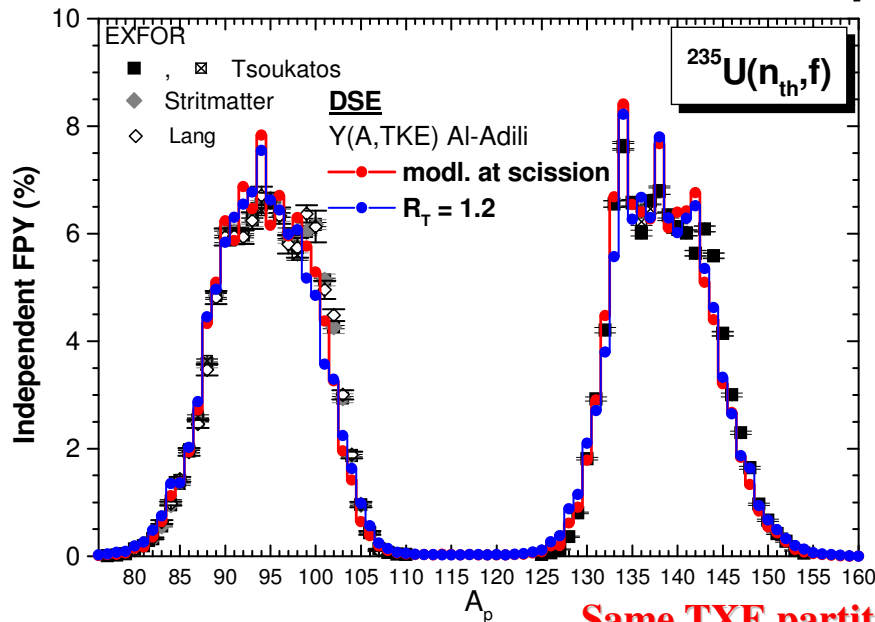
Influence of  $Y(A, TKE)$  on  $Y(A_p) \rightarrow Y(A_p)$  reflects the behaviour of  $Y(A)$



The use of different  $Y(A, TKE)$  data does not change the position of peaks and dips in the  $Y(A_p)$  structure (e.g. pronounced peaks at  $A_p = 134, 138, 94, 90$ , and dips at  $A_p = 136, 141, 97$ ) only their magnitude is changed.



## Influence of TXE partition on $Y(A_p)$

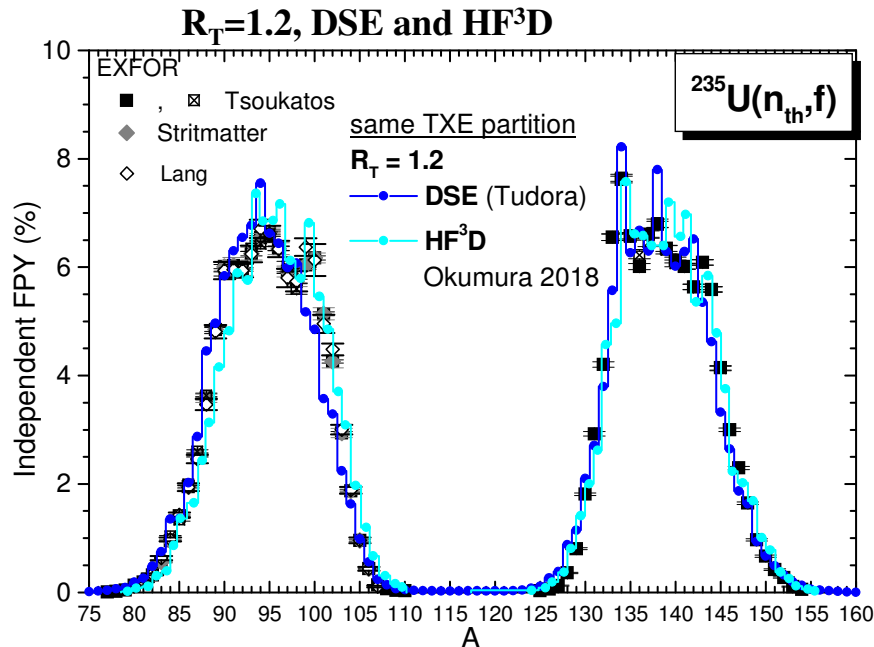


← **Same model, different TXE partitions**

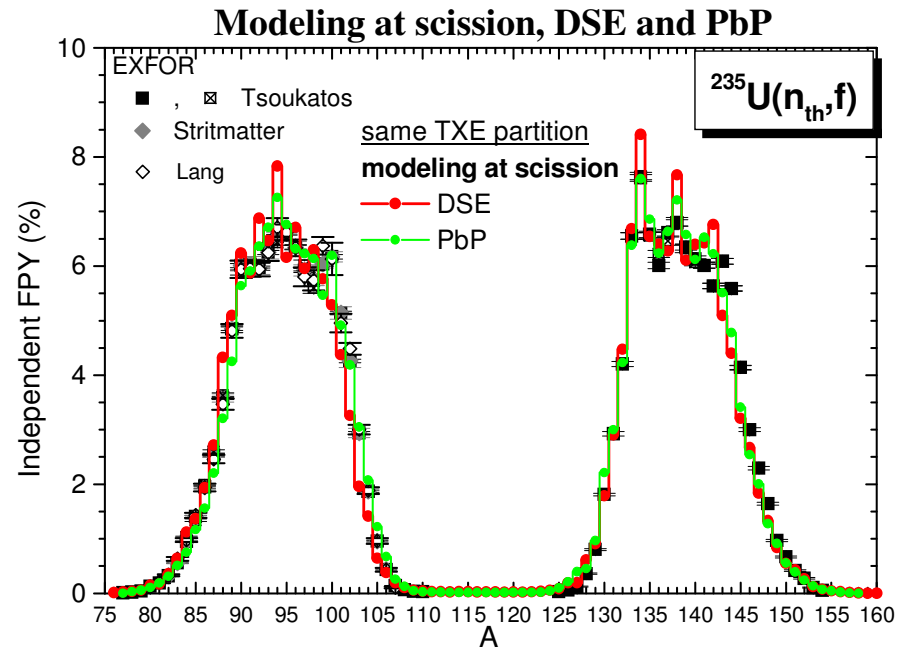
The position of pronounced peaks at e.g.  $A_p = 134, 138, 94, 90$ ) and dips at e.g.  $A_p = 136, 97, 141$  *remains the same*.

But the position of other peaks and dips which are less pronounced is changing, so that some differences in the  $Y(A_p)$  structure are seen (especially in the case of light fission products).

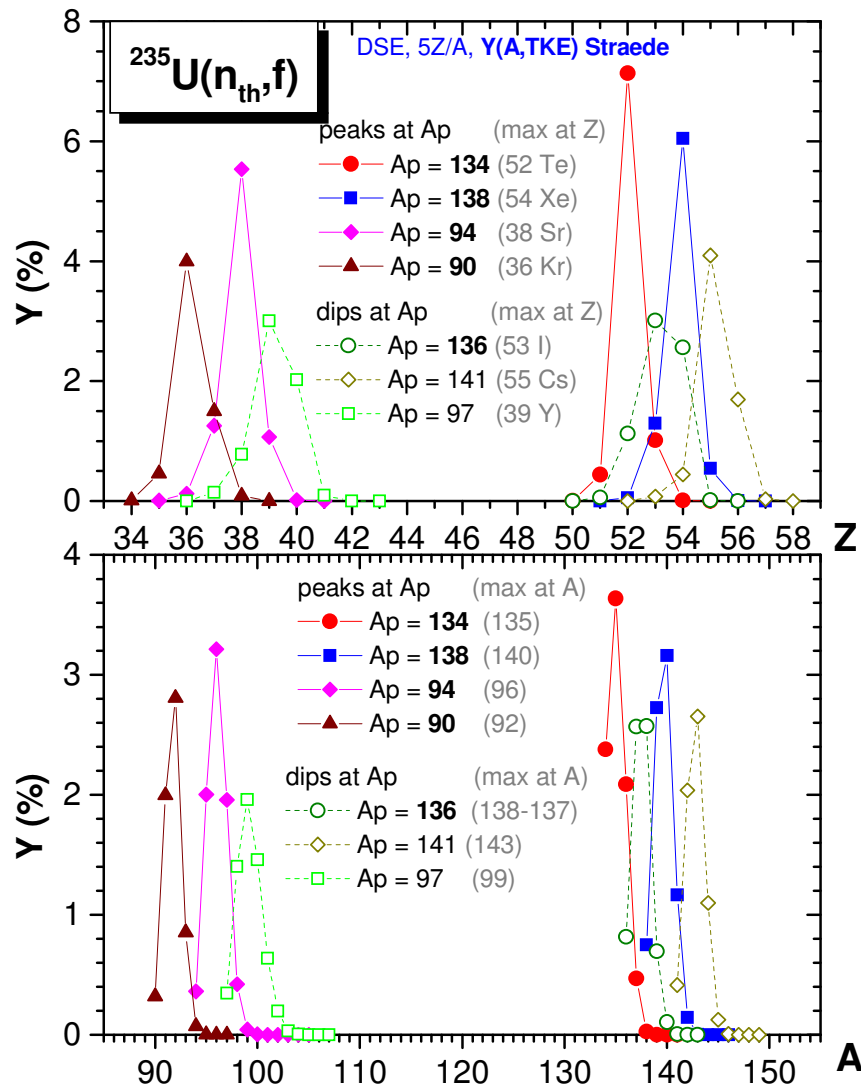
**Same TXE partition and different models:**



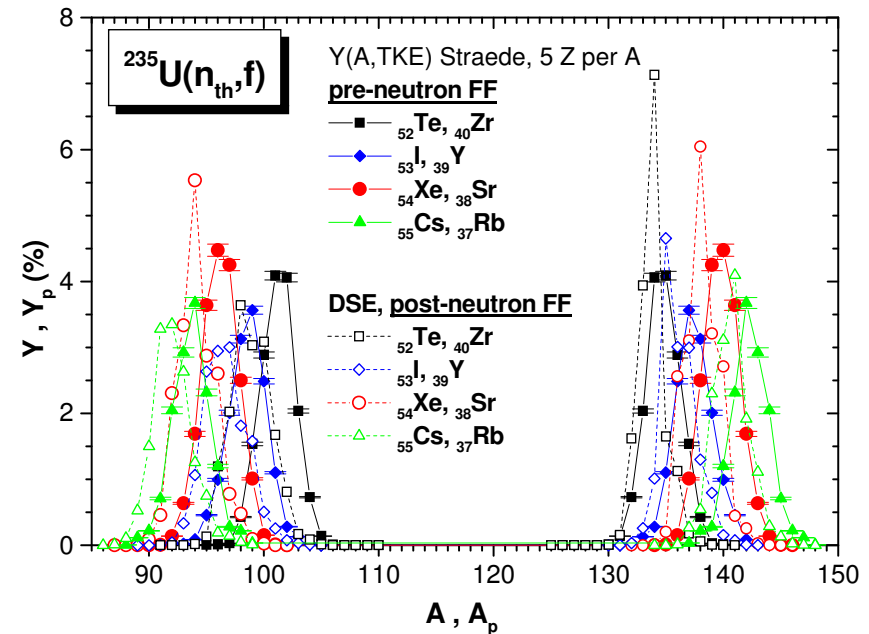
The position of less pronounced peaks and dips is changing → some differences in the  $Y(A_p)$  structure are seen



**Charge and mass distrib of pre-neutron fragments which lead to pronounced peaks and dips at  $A_p$  values (indicated in bold)**



**Pre- and post-neutron fragm. distributions  $Y(Z,A)$  (full symbols) and  $Y(Z,A_p)$  (open symbols) for the charge pairs indicated in the figure.**



These figures show that:

- The most probable pre-neutron fragments leading to **peaks** in the  $Y(A_p)$  structure are either **even-even** nuclei ( $^{140}\text{Xe}$ ,  $^{96}\text{Sr}$ ,  $^{92}\text{Kr}$ ) or **even-odd** nuclei ( $^{135}\text{Te}$ ).
- While the pronounced dips are coming from **odd-Z** pre-neutron fragments (e.g.  $^{143}\text{Cs}$ ,  $^{137,136}\text{I}$ ,  $^{99}\text{Y}$ ).

**This fact highlights again the important role of the even-odd effect in fragment charge**

# Conclusions

The  $Y(Z, A_p)$  and  $Y(A_p)$  results **describe reasonably well** the experimental data (EXFOR).

➤ **Influence on independent FPY (post-neutron fragment yields  $Y(Z, A_p)$ ,  $Y(A_p)$ ):**

• **of TXE partition** → in the  $Y(A_p)$  structure: the position of pronounced peaks (e.g. at  $A_p = 134, 138, 94$ ) and dips (e.g.  $A_p = 136, 141, 97$ ) does not change. The position of other less pronounced peaks and dips is changing being influenced by the TXE partition.

• **of  $Y(A, TKE)$**  → only in the magnitude of peaks and dips in  $Y(A_p)$ , reflecting the behaviour of  $Y(A)$ . The position of peaks and dips is not influenced by  $Y(A, TKE)$ .

The pronounced peaks in  $Y(A_p)$  e.g. at  $A_p = 134, 139, 94$  are due to even-Z fragments  $^{135}_{52}\text{Te}$ ,  $^{140}_{54}\text{Xe}$ ,  $^{96}_{38}\text{Sr}$ , while the pronounced dips e.g. at  $A_p = 141, 136, 97$  are due to odd-Z fission fragments  $^{143}_{55}\text{Cs}$ ,  $^{137}_{53}\text{I}$ ,  $^{99}_{39}\text{Y}$ .

This fact highlights again **the important role of the even-odd effect in fragment charge**.

The influence on other post-neutron fragment distributions was investigated in a recently published paper: *A. Tudora, Eur.Phys.J.A 58 (2022) 126*, leading to the following conclusions:

➤ **Influence on the isotonic yield of post-neutron fragments  $Y(N_p)$ :**

- **of TXE partition** → similar to that on independent FPY  $Y(A_p)$  but less pronounced.
- **of  $Y(A, TKE)$**  is almost insignificant

➤ **Influence on the kinetic energy distributions of post-neutron fragments:**

- **of TXE partition** is very low
- **of  $Y(A, TKE)$**  → the behaviour of  $KE_p(A)$ ,  $KE_p(Z)$ ,  $TKE_p(Z)$  reflect the differences existing between the kinetic energy distributions of pre-neutron fragments  $KE(A)$ ,  $KE(Z)$ ,  $TKE(Z)$ .



## Influence of energy partition in fission and pre-neutron fragment distributions on post-neutron fragment yields, application for $^{235}\text{U}(n_{\text{th}},f)$

Anabella Tudora<sup>a</sup>

University of Bucharest, Faculty of Physics, str. Atomistilor 405, Magurele, POB MG-11, 77125 Bucharest, Romania

Received: 30 April 2022 / Accepted: 10 June 2022

© The Author(s), under exclusive licence to Società Italiana di Fisica and Springer-Verlag GmbH Germany, part of Springer Nature 2022

Communicated by Cedric Simenel.

**Abstract** The key role in the calculation of post neutron fragment yields (independent fission product yields FPY) is played by (a) the pre-neutron fragment distributions  $Y(A,Z,TKE)$  and (b) the prompt neutron multiplicity (calculated in the frame of a prompt emission model). The knowledge of excitation energies of fully accelerated fragments is crucial in any modeling of prompt emission. Consequently in this paper the influence on independent FPY and kinetic energy distributions of post neutron fragments of both the pre-neutron fragment distribution and the partition of total excitation energy (TXE) is investigated. To do that, two reliable experimental  $Y(A,TKE)$  distributions of the standard fissioning nucleus  $^{235}\text{U}(n_{\text{th}},f)$  and two methods of TXE partition are considered. Nowadays two types of TXE partitions are employed in different prompt emission models, i.e. energy partitions based on different modelings at scission and different parameterizations which allow the TXE sharing by avoiding what is happening at scission. For this reason the methods of TXE partition chosen in this work belong to both types, i.e. (i) the TXE partition based on modeling at scission used in the deterministic prompt emission models PbP and DSE and (ii) the TXE partition according to the temperature ratio  $R_T = T_L/T_H$  of complementary fully accelerated fragments (employed in the deterministic HE<sup>3</sup>D model and the

and  $N_p = 83$ , respectively) only their magnitude is influenced by  $Y(A,TKE)$  distribution, while the TXE partition influences the position of less pronounced peaks and dips in the structures of  $Y(A_p)$  and  $Y(N_p)$ . The TXE partition has an insignificant influence on different kinetic energy distributions of post-neutron fragments, while the differences existing between the kinetic energy distributions of pre-neutron fragments are reflected in the kinetic energy distributions of post-neutron fragments.

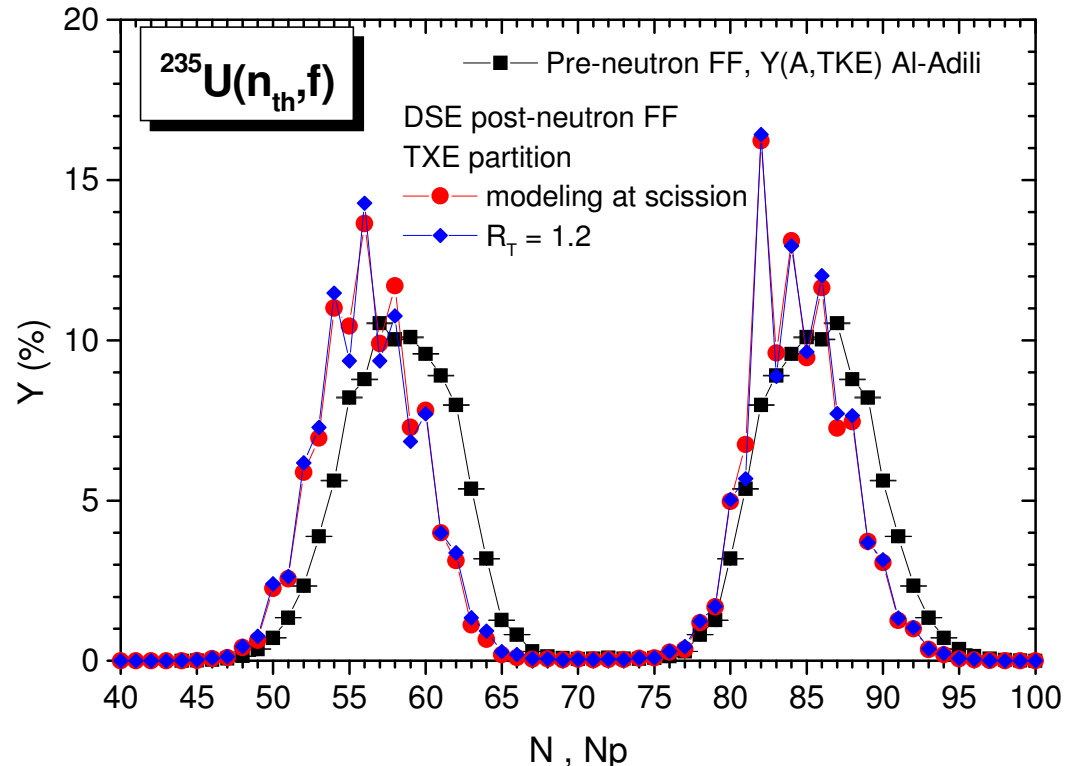
### 1 Introduction

Compared to the pre-scission stage which includes only one nucleus undergoing fission (with its complicate evolution along the fission path, from the initial deformation up to the final deformation and its rupture) treated in competition with other reaction channels, the post-scission stage of fission includes many nuclei (named fission fragments or pre-neutron fission fragments), resulting from a very large variety of splits (the binary fission being the most probable) going from symmetric fission up to very asymmetric fragmentations.

The fission fragments (characterized by their distribution

Other slides (eventual completions)

## Isotonic yield of post-neutron fragments $Y(N_p)$



-the influence of  $Y(A, TKE)$  on  $Y(N_p)$  is almost insignificant (only the case  $Y(A, TKE)$  Al-Adili is plotted)

-the influence of TXE partition on  $Y(N_p)$  is similar to that on  $Y(A_p)$  but it is lower.

(i.e. the position of pronounced peaks and dips in the  $Y(N_p)$  structure does not change, only the position of less pronounced peaks and dips is changing).

- The most pronounced peak at  $N_p = 82$  (magic number) correspond to the most pronounced peak in  $Y(A_p)$  at  $A_p = 134$  being due to the post-neutron fragment  $^{134}\text{Te}$  (resulting from the initial fragment  $^{135}\text{Te}$ )
- Other peaks in  $Y(N_p)$  located e.g. at  $N_p = 84, 56$  correspond to the peaks in  $Y(A_p)$  located at  $A_p = 138, 94$  being due to the post-neutron fragments  $^{138}\text{Xe}, ^{94}\text{Sr}$  (resulting from the initial fragments  $^{140}\text{Xe}, ^{96}\text{Sr}$ )
- The pronounced dip at  $N_p = 83$  correspond to the dip in  $Y(A_p)$  placed at  $A_p = 136$  being due to the post-neutron fragment  $^{136}\text{I}$  (resulting from the initial fragments  $^{138, 137}\text{I}$ )

## Different kinetic energy distributions of post-neutron fragments

**DSE approach** – allows to calculate the kinetic energy of each residual fragment

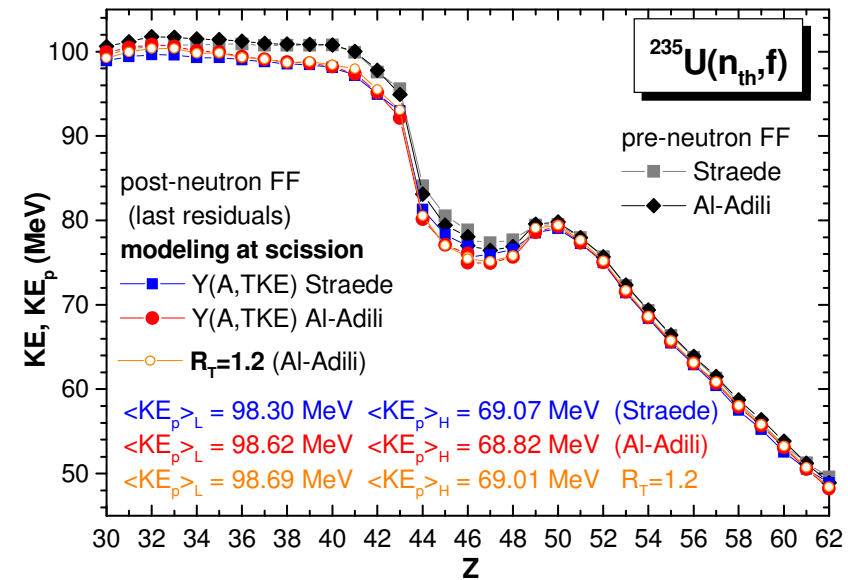
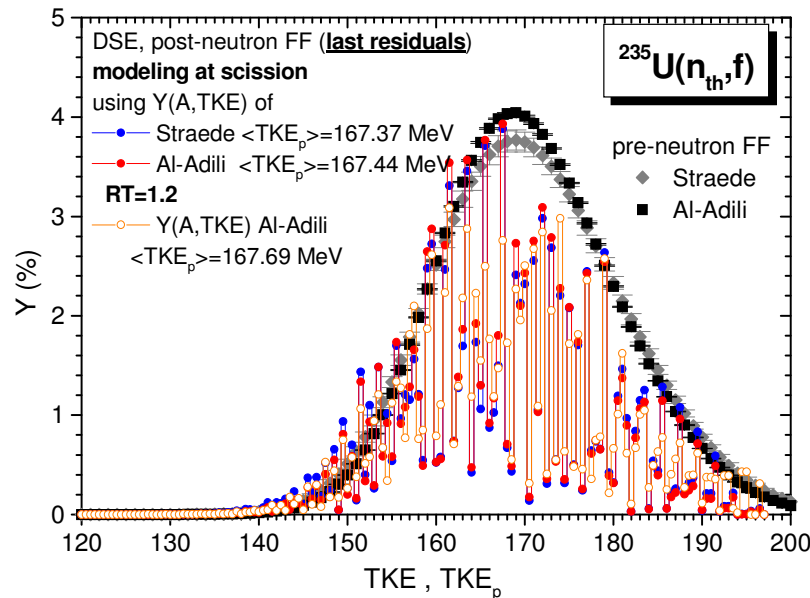
following the successive emission of each prompt neutron, the emission sequence  $k = 1$  to  $n(A, Z, TKE)$  :

$$KE_k(A, Z, TKE) = (A - k) KE(A, Z, TKE) / A$$

- kinetic energy of **the last residual fragment** (fission product) with the mass number  $A_p = A - n(A, Z, TKE)$

$$KE_{p_{last}}(A, Z, TKE) = (A - n(A, Z, TKE)) KE(A, Z, TKE) / A$$

**Low influence** of both the TXE partition and  $Y(A, TKE)$  on  $Y(TKE_p)$ ,  $KE_p(Z)$ ,  $KE_p(A_p)$  etc.



This low influence is well reflected in the total average values (first moments of these distributions) e.g.  $\langle TKE_p \rangle$ ,  $\langle KE_p \rangle_{L,H}$  which differ from each other with **less than 1%** in all 4 studied cases (2 methods of TXE partition and 2 pre-neutron fragment distributions  $Y(A, TKE)$ ).



$\langle KE_p \rangle_L$ (MeV)		$\langle KE_p \rangle_H$ (MeV)		$\langle TKE_p \rangle$ (MeV)		TXE partition	Y(A, TKE)
last resid.	average	last resid.	average	last resid.	average		
98.617	99.087	68.819	68.946	167.436	168.032	Modl. sciss.	Al-Adili
98.304	98.800	69.066	69.198	167.370	167.998	Modl. sciss.	Straede
98.685	99.192	69.010	69.113	167.695	168.304	$R_T = 1.2$	Al-Adili
98.424	98.956	69.265	69.401	167.718	168.357	$R_T = 1.2$	Straede

**DSE:** kinetic energy of each residual fragment following the successive emission of each prompt neutron, the emission sequence  $k = 1$  to  $n(A, Z, TKE)$  :

$$KE_k(A, Z, TKE) = (A - k) KE(A, Z, TKE) / A$$

➤ kinetic energy of **the last residual fragment** (fission product) with the mass number  $A_p = A - n(A, Z, TKE)$

$$KE_{p_{last}}(A, Z, TKE) = (A - n(A, Z, TKE)) KE(A, Z, TKE) / A$$

➤ as an *average over the emission sequences*:

$$KE_{p_{av}}(A, Z, TKE) = \frac{1}{n(A, Z, TKE)} \sum_{k=1}^{n(A, Z, TKE)} KE_k(A, Z, TKE)$$

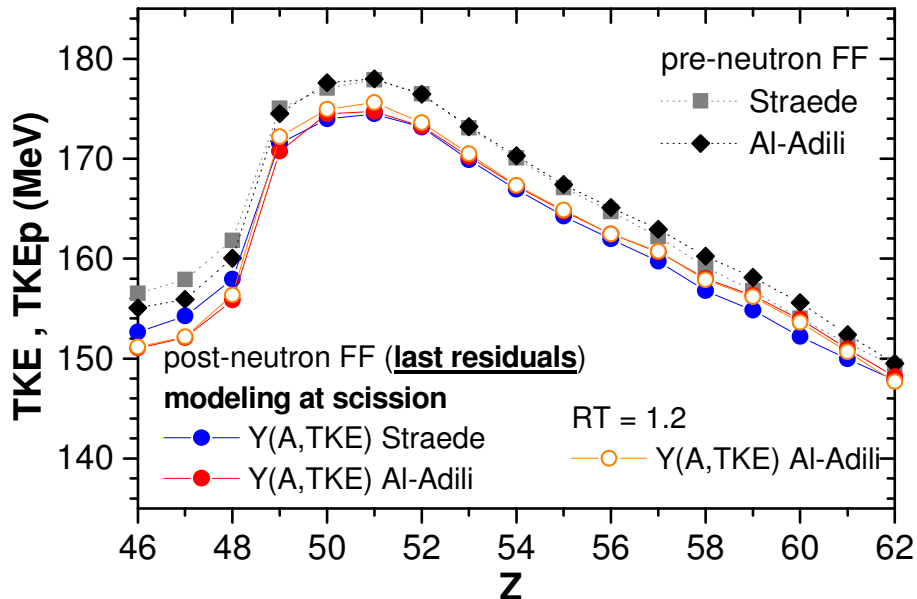
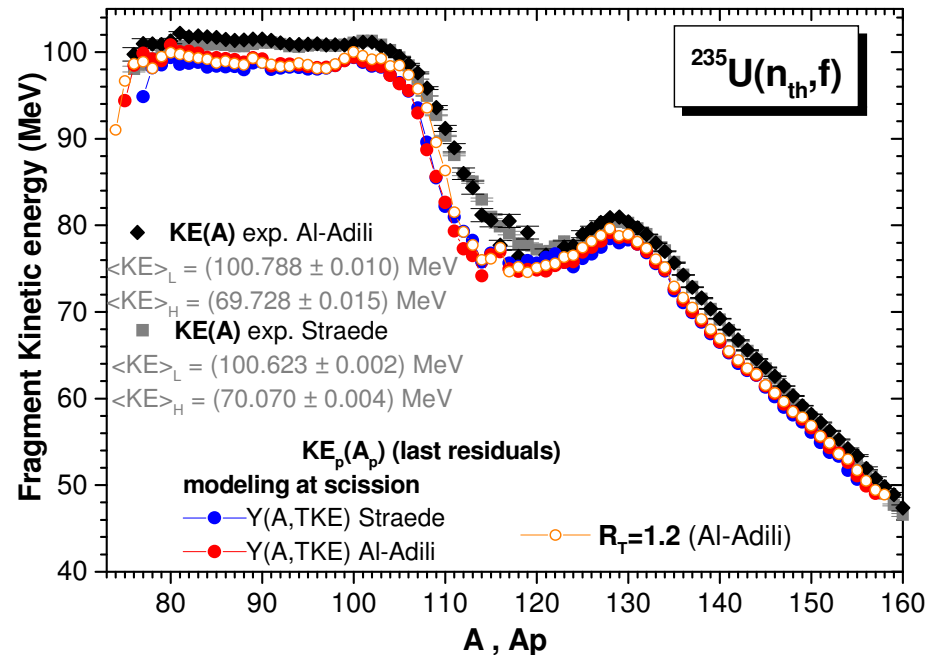
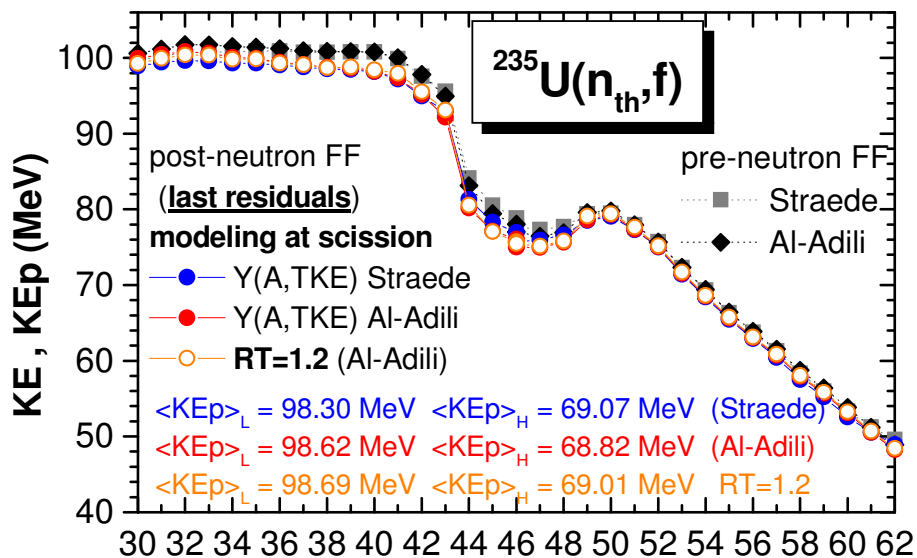


Which is similar to the cases:

- only experimental  $\nu(A)$  and  $TKE(A)$  are available  
 $KE_p(A) = KE(A)(1 - \nu(A) / A)$
- PbP: the  $\nu(A, Z, TKE)$  matrix as an average over the emission sequences  
 $KE_p(A, Z, TKE) = KE(A, Z, TKE)(1 - \nu(A, Z, TKE) / A)$

$TKE_p$ : as a sum of  $KE_p$  corresponding to complementary initial fragments:

$$TKE_{p_{last/av}}(A, Z, TKE) = KE_{p_{last/av}}(A, Z, TKE) + KE_{p_{last/av}}(A_F - A, Z_F - Z, TKE)$$



- Low influence of TXE partition on KE<sub>p</sub> and TKE<sub>p</sub> (compare the full red and open orange symbols)
- Influence of Y(A,TKE) → the differences between the distributions of post neutron kinetic energies reflect the differences existing between the kinetic energy distributions of initial fragments. (compare the red and blue symbols and the black and gray symbols)